

PROCEEDINGS

AMERICAN SOCIETY OF CIVIL ENGINEERS

AUGUST, 1954



EQUATION OF THE FREE-FALLING NAPPE

by Fred W. Blaisdell, M. ASCE

HYDRAULICS DIVISION

{Discussion open until December 1, 1954}

*Copyright 1954 by the AMERICAN SOCIETY OF CIVIL ENGINEERS
Printed in the United States of America*

Headquarters of the Society

33 W. 39th St.
New York 18, N. Y.

PRICE \$0.50 PER COPY

THIS PAPER

--represents an effort by the Society to deliver technical data direct from the author to the reader with the greatest possible speed. To this end, it has had none of the usual editing required in more formal publication procedures.

Readers are invited to submit discussion applying to current papers. For this paper the final date on which a discussion should reach the Manager of Technical Publications appears on the front cover.

Those who are planning papers or discussions for "Proceedings" will expedite Division and Committee action measurably by first studying "Publication Procedure for Technical Papers" (Proceedings — Separate No. 290). For free copies of this Separate—describing style, content, and format—address the Manager, Technical Publications, ASCE.

Reprints from this publication may be made on condition that the full title of paper, name of author, page reference (or paper number), and date of publication by the Society are given.

The Society is not responsible for any statement made or opinion expressed in its publications.

This paper was published at 1745 S. State Street, Ann Arbor, Mich., by the American Society of Civil Engineers. Editorial and General Offices are at 33 West Thirty-ninth Street, New York 18, N. Y.

EQUATION OF THE FREE-FALLING NAPPE

Fred W. Blaisdell,¹ M. ASCE

SYNOPSIS

A general equation for the form of the nappe is developed in this paper. The equation is not valid close to the crest, but applies to that portion of the nappe that is free-falling—where pressures within the nappe are atmospheric. The constants in the equation have been evaluated for the vertical, sharp-crested weir having approach channel depths ranging from deep to zero (the free overfall); that is, over the entire range of subcritical approach velocities. The evaluation is made using nappe coordinates obtained by others. The equation is checked by comparing its predictions with a number of published profiles. The comparison is shown to be excellent for the lower approach velocities and good at the higher approach velocities.

INTRODUCTION

An adequate number of carefully performed experiments already have been made and published which give the form of the nappe produced by a vertical sharp-crested weir. It would seem that any further writings on the subject would be superfluous. However, no general equation for the form of the nappe that covers velocities of approach other than zero has been derived from the experimental data.

The need for a general equation for the form of the nappe became apparent when the writer and his colleagues were assigned the task of developing a design for a stilling basin for use with straight drop spillways. This is because it is desirable to use general formulas for the determination of the component dimensions when developing generalized designs. The straight drop spillway is ordinarily a vertical weir over which water falls onto an apron on which energy is dissipated. The point at which the nappe strikes the apron is important since this in some measure determines the location of the blocks and sills used to assist the energy dissipation. It is also a factor in the determination of the basin length.

1. Project Supervisor, U. S. Department of Agriculture, ARS, St. Anthony Falls Hydraulic Laboratory, Minneapolis, Minnesota.

Scope

The study reported here has resulted in the development of a general formula for the trajectory of the lower and upper nappes of a vertical sharp-crested weir with velocity of approach (or approach channel depth) as a variable. The equation applies only to that portion of the nappe which is free-falling, that is, where the pressure at every point within the nappe is atmospheric. The equation is valid for approach velocities ranging from zero to the critical velocity.

It is well known that convergence of the streamlines causes the pressure within the nappe to be greater than atmospheric for a short distance downstream of the crest. The formula presented here represents a parabolic curve. This curve form is produced when the only force acting on the nappe is that of gravity. Therefore, the formula is not valid in the vicinity of the weir crest where pressures within the nappe are above atmospheric. The lower limit of the applicability of the equation is at $x/H \approx 0.5$. Here x is the abscissa measured from the upstream face of the weir and H is the specific head.

Works Utilized

Data obtained from a number of different sources were analyzed by the writer.

Probably the best known nappe coordinates that are used here are those which William P. Creager (1),² Hon. M. ASCE, extrapolated from Bazin's experiments. Bazin's data extended only about to $x/H = 0.12$ for the upper nappe and to about $x/H = 0.65$ for the lower nappe. This is probably within the range of positive pressures within the nappe. Mr. Creager extended the nappe by considering the horizontal velocity to be constant and the vertical velocity to increase under the influence of gravity. His lower nappe formula for the vertical weir with zero approach may be written

$$\frac{y}{H} = 0.190 + 0.046\left(\frac{x}{H}\right) - 0.366\left(\frac{x}{H}\right)^2 \quad (1)$$

where y is the ordinate measured from the weir crest. Positive values of y are above the crest level, negative values below.

The Bureau of Reclamation (2) of the U. S. Department of the Interior conducted a most thorough and detailed study of the nappe form. Their data were analyzed by plotting the nappe coordinates to a large scale, drawing a smooth curve through the data, reading coordinates from the curve and dividing by H , combining the coordinates according to h_v/H , plotting the coordinates for each value of h_v/H , drawing an average curve through this data, reading coordinates from this average curve,

2. Numerals in parentheses, thus: (1), refer to corresponding items in the Bibliography (see Appendix).

and tabulating the readings. Here h_v is the velocity head in the approach channel. The data given in Tables 12 and 18 of Reference (2) were used by the writer.

Hinds, Creager, and Justin (3) present a table of nappe coordinates for various approach velocities. Their table was adapted from a thesis by Jacob E. Warnock (4), M. ASCE. Mr. Warnock's thesis was based on the Bureau of Reclamation data mentioned previously. The close agreement between the two sets of data that later will become apparent is therefore not surprising.

Calvin V. Davis (5), M. ASCE, also presents a table of nappe coordinates for vertical sharp-crested weirs. The data on which this table is based were obtained by the Bureau of Reclamation, M. Bazin, and Professor Scimemi. In a letter to the writer, Mr. E. W. Lane, M. ASCE, who prepared the table, states that the data he used were not the Bureau of Reclamation data mentioned previously. It was data obtained at an earlier date. It may, therefore, be considered as distinct from the other Bureau of Reclamation data.

Ettore Scimemi (6), M. ASCE, has published experimental data obtained on a vertical sharp-crested weir. The particular value of Professor Scimemi's presentation is that his nappe coordinates cover a much wider range than does any other data that the writer has been able to discover. For the lower nappe, Professor Scimemi gives an equation which can be written

$$\frac{y}{H} = 0.182 - 0.054\left(\frac{x}{H}\right) - 0.416\left(\frac{x}{H}\right)^2 \quad \text{for } \frac{x}{H} > 0.50 \quad (2a)$$

while for the upper nappe

$$\frac{y}{H} = -0.243 + 0.694\left(\frac{x}{H}\right) - 0.496\left(\frac{x}{H}\right)^2 \quad \text{for } \frac{x}{H} > 1.40 \quad (2b)$$

A. T. Ippen (7), M. ASCE, shows the form of the nappe in his Fig. 11, p. 529 (this figure was originally presented by Hunter Rouse (8), M. ASCE) and gives a chart of nappe coordinates in his Figs. 12, pp. 530-531. Fig. 11 gives the nappe form for four approach channel depths. The coordinates of these nappes were scaled from the figure. In addition, coordinates of the nappe were read from Figs. 12 for a number of approach channel depths which were subsequently converted to approach velocity heads. The data obtained from each of these figures were used by the writer.

The final group of data used by the writer was unpublished information obtained by Donald A. Parsons, a former colleague of the writer. Mr. Parsons' data apply to the free overfall only.

Method of Analysis

In common with Mr. Creager, Dr. Ippen, and others, the writer makes the reasonable assumptions that the horizontal velocity is

constant and that the only force acting on the nappe is gravity g . A particle of water in the lower nappe³ will, in the time t , travel a horizontal distance x from the face of the weir of

$$x = v_0 t \cos \theta \quad (3)$$

In the same time the particle will travel a vertical distance y of

$$y = C' + v_0 t \sin \theta + \frac{1}{2} g t^2 \quad (4)$$

In Eqs. 3 and 4 v_0 is the velocity, θ is the angle of inclination of the velocity with the horizontal at the point where $x = 0$, and C' is the value of y at $x = 0$. Solving Eq. 3 for t , substituting in Eq. 4, and simplifying

$$y = C' + x \tan \theta + \frac{g}{2 v_0^2 \cos^2 \theta} x^2 \quad (5)$$

Eq. 5 gives the form of the lower nappe.

Since the horizontal velocity is constant the vertical thickness of the nappe T must also be constant. The equation of the upper nappe is then

$$y = C' + x \tan \theta + \frac{g}{2 v_0^2 \cos^2 \theta} x^2 + T \quad (6)$$

It is advantageous when developing a general formula to use dimensionless units. The basic unit of measurement will be the specific head H . This is the total head over the weir—the observed head plus the velocity head. Dividing both sides of Eqs. 5 and 6 by H and substituting C for C'/H , and S for $gH/v_0^2 \cos^2 \theta$ the equation for the lower nappe is

$$\frac{y}{H} = C + \frac{x}{H} \tan \theta + \frac{S}{2} \left(\frac{x}{H} \right)^2 \quad (7)$$

and for the upper nappe

$$\frac{y}{H} = C + \frac{x}{H} \tan \theta + \frac{S}{2} \left(\frac{x}{H} \right)^2 + \frac{T}{H} \quad (8)$$

Eqs. 7 and 8 are the basic equations used in this analysis.

3. It is not necessary to specify any particular part of the nappe because the development is completely general. The lower nappe is specified here because its form is desired initially.

The method of analyzing the data was suggested by Donald A. Parsons. It is so simple and such a useful tool that it is surprising that apparently no previous use has been made of it, at least so far as the writer can deduct from the available publications.

Differentiating Eq. 7 and rearranging

$$\frac{d(y/H)}{d(x/H)} = \tan \theta + S \left(\frac{x}{H} \right) \quad (9)$$

An identical result is obtained on differentiating Eq. 8. This indicates that coordinates of both the upper and lower nappes may be used to evaluate $\tan \theta$ and S . Steps in the analysis included: (1) reducing observed values of x and y to x/H and y/H ; (2) computing $\Delta(x/H)$, $\Delta(y/H)$, and $\frac{\Delta(y/H)}{\Delta(x/H)}$; (3) plotting $\frac{\Delta(y/H)}{\Delta(x/H)}$ vs. x/H as in Fig. 1; fitting a curve (a straight line) to the plotted points; and (4) determining S from the slope of the curve and $\tan \theta$ from the intercept of the curve at $x/H = 0$. The constant C was computed for each plotted point by substituting $\tan \theta$ and S in Eq. 7.

The scale of the plots made it difficult to read $\tan \theta$ and S as precisely as was desired. Therefore, C was plotted against x/H and $(x/H)^2$ to check $\tan \theta$, S , and C . A typical plot for the data appearing in Fig. 1. is shown in Fig. 2. The slope in Fig. 2a indicates that $\tan \theta$ was read incorrectly and that its true value is 0.085 instead of 0.08 as was read originally. Also from Fig. 2a the correct value of C is seen to be 0.139. If the data in Fig. 2a had curved systematically it would have indicated an error in S . The plot of Fig. 2b has been prepared to indicate that S is satisfactory after correcting $\tan \theta$. The waviness of the data in Figs. 1 and 2 is an indication that the Bureau of Reclamation table, in spite of the care lavished on it, is still somewhat rough. Mr. Lane smoothed his table by computing second differences and his results do not exhibit the scatter shown in Figs. 1 and 2.

The nappe thickness T was computed by subtracting the upper nappe coordinates from the lower nappe coordinates and averaging the results. The variation from the average was not great until the nappe surface appeared to break up and accurate surface readings became difficult. The average nappe thickness between x/H values of 0.5 and 1.8 is the figure recorded for the Bureau of Reclamation and the Hinds, Creager, Justin data. For the other data employed, the nappe thickness was computed for values of $x/H > 0.5$.

The equations given in this paper are valid only at values of $x/H > 0.5$. This is a conservative general statement. The plotted data indicate that the equation may be valid at lower values of x/H for the lower nappe than for the upper nappe.

The reason why the equation is not valid between x/H values of 0 and about 0.5 is apparent after considering the difference between the original assumption of atmospheric pressure within the nappe and the actual condition existing near the crest. Professor Scimemi's (6) experimental results show that pressures within the nappe are greater than atmospheric to $0.5x/H$ but that at about this point they become

negligible and that they disappear at higher values of x/H . Therefore, it is not to be expected that the equations developed here will be valid close to the weir crest.

A physical illustration of the meaning of the constants in Eq. 7 will perhaps be helpful. The constants C and $\tan \theta$ are illustrated in Fig. 3a. There it can be seen that C is the intercept of y/H at the plane of the weir crest. The value of C would be zero if the nappe were free-falling at the weir crest. The nappe is under the influence of converging streamlines at the crest and is not free-falling. Thus C has a value other than zero except for the case of the free overfall where C approaches zero. The constant C is found, as was mentioned previously, by substituting in Eq. 7 after $\tan \theta$ and S had been evaluated. Also the controlling streamline at the plane of the weir crest is not horizontal. For the vertical weir, it is inclined slightly upward while for the free overfall it is inclined downward. The inclination is illustrated in Fig. 3a and its magnitude is found by projecting the slope of the free-falling nappes, shown in Fig. 3b, back to the plane of the weir crest. The slope, $\tan \theta$, can also be found by substituting in Eq. 9 after S has been evaluated.

The vector diagram of Fig. 3c explains S . The velocity vectors at points 1 and 2 in Fig. 3a are transferred to Fig. 3c. The change in velocity direction between points 1 and 2 is a result of the influence of gravity acting on the vertical component of the velocity, since an original assumption was that the horizontal component of the velocity was constant. The vertical acceleration, represented by S , was actually determined from the slope of the curve of Fig. 3b. It could have been determined also by computing the second differential of Eqs. 7 or 8 which is

$$\frac{d^2 (y/H)}{d (x/H)^2} = S \quad (10)$$

Results of Analysis

Form of the Nappe for Zero Velocity of Approach

More data are available for the vertical weir having a zero velocity of approach than for other approach velocities. It is therefore possible to provide a more reliable determination of the constants in Eq. 7 for this condition than for other velocities of approach. The original data for each of the lower nappe profiles were first plotted so they might be compared. These are shown in Fig. 4. It will be noted that the profiles compare well except for the Davis (Reference (5), p. 338, Table 1) and the Creager (Reference (1), Fig. 25) profiles. The Davis curve falls below the other curves. Since the Bureau of Reclamation data on which this curve is largely based were superseded by data obtained later by the same Bureau, the Davis coordinates were not used in computing values of the constants. The Creager data fall above the other curves. Since these coordinates were projected by Creager from data by Bazin that extended only to $x/H \approx 0.65$, they too were

not averaged. In this connection, Mr. Creager (1), p. 110, notes, "The paths are only approximate, as they are extended from experimental points relatively close to the top of the dam. . ."

The values of C , $\tan \theta$, $S/2$, and T determined from the various data are given in Table 1. The averages for the Scimemi; Hinds, Creager, and Justin; Bureau of Reclamation; and Ippen data are also given. Also listed are values of the constants which the author proposes as being even values that are close to the average. The curve in Fig. 4 is plotted using these proposed values. The excellent agreement with the observed data is obvious.

Effect of Approach Velocity

Increasing the velocity of approach causes reductions in C , in $\tan \theta$, and in the effect of gravity. The effect is shown in Fig. 5 where C , $\tan \theta$, $S/2$, and T are plotted against the relative velocity head h_v/H . Only the Bureau of Reclamation; Hinds, Creager, and Justin; and Ippen give nappe coordinates for different approach velocities. The trend of the data was established by the plotted points. The initial point on each curve was established by the proposed value given in Table 1. The equations for the four constants in Eqs. 7 and 8 are

$$C = 0.150 - 0.45\left(\frac{h_v}{H}\right) \quad (11)$$

$$\tan \theta = 0.411 - 1.603\left(\frac{h_v}{H}\right) - \sqrt{1.568 \left(\frac{h_v}{H}\right)^2 - 0.892\left(\frac{h_v}{H}\right) + 0.127} \quad (12)$$

$$\frac{S}{2} = -0.425 + 0.25\left(\frac{h_v}{H}\right) \quad (13)$$

and

$$\frac{T}{H} = 0.57 - \frac{(10m)^2 e^{10m}}{50} \quad (14)$$

where $m = (h_v/H) - 0.208$. Substituting these values in Eqs. 7 and 8 gives the general equations for the lower and upper nappes for the vertical weir. The equations are, for the lower nappe,

$$\begin{aligned} \frac{y}{H} = & 0.150 - 0.45\left(\frac{h_v}{H}\right) + \left[0.411 - 1.603\left(\frac{h_v}{H}\right) \right. \\ & \left. - \sqrt{1.568\left(\frac{h_v}{H}\right)^2 - 0.892\left(\frac{h_v}{H}\right) + 0.127} \right] \frac{x}{H} \\ & + \left[-0.425 + 0.25\left(\frac{h_v}{H}\right) \right] \left(\frac{x}{H}\right)^2 \end{aligned} \quad (15)$$

and, for the upper nappe,

$$\begin{aligned} \frac{y}{H} = & 0.150 - 0.45\left(\frac{h_v}{H}\right) + \left[0.411 - 1.603\left(\frac{h_v}{H}\right) \right. \\ & \left. - \sqrt{1.568\left(\frac{h_v}{H}\right)^2 - 0.892\left(\frac{h_v}{H}\right) + 0.127} \right] \frac{x}{H} \\ & + \left[-0.425 + 0.25\left(\frac{h_v}{H}\right) \right] \left(\frac{x}{H}\right)^2 + 0.57 - \frac{(10m)^2}{50} \frac{10m}{50} \end{aligned} \quad (16)$$

These equations are valid only for $x/H > 0.50$ and for values of h_v/H between 0 and $1/3$ —the subcritical velocity range of flow.

Comparison with Published Nappes

The proof of Eqs. 15 and 16 is in the comparison of their predictions with the published nappe profiles. The comparison for $h_v/H = 0$ is shown in Fig. 4 to be excellent. Comparisons for $h_v/H = 0.10, 0.20$, and 0.33 are shown in Fig. 6. The comparisons in general are seen to be very good. Only at $h_v/H = 0.319$ was the comparison poor (not shown). There is need for more data between relative velocity heads of 0.2 and 0.33 to better define the equation between these limits; the equation admittedly needs additional verification within this range.

Nappe Form for $0 < x/H < 0.5$

It has been noted previously that Eqs. 7 and 8 or Eqs. 15 and 16 are not valid when x/H is less than about 0.5 . If the form of the nappe is needed below $x/H = 0.5$ it is necessary to obtain it from some other source. It is suggested that the coordinates be obtained from one of

the sources that have shown good agreement with the equations in Figs. 4 and 6. Some slight adjustment may be required to insure that the two curves join perfectly, but no adjustments that would cause any concern are anticipated.

SUMMARY

Eqs. 15 and 16 give the form of the nappe which falls freely from a vertical, sharp-crested weir. The nappe is free-falling beyond about $0.5H$ from the weir crest. The equations are valid for approach velocities lying within the entire subcritical velocity range; they are valid for approach channel depths ranging from deep to zero below the weir crest.

The equations give excellent agreement with experimental data for the lower approach velocities and good agreement for all but one of the higher approach velocities.

COMMENT

The fact that the equations are not valid in the vicinity of the crest may be considered a serious deficiency by some persons. It should be remembered that they were not developed to give the form of a dam face, although Eq. 15 can be used for this purpose. The equations were developed to give the point at which the free-falling nappe hits the apron in order to provide one of the dimensions necessary for the determination of the apron length.

ACKNOWLEDGMENTS

The work reported here was initiated as part of a study leading to the development of a generalized design for straight drop spillways. It was carried out by the staff of the Soil Conservation Service of the U. S. Department of Agriculture located at the St. Anthony Falls Hydraulic Laboratory of the University of Minnesota and was done under a cooperative agreement between the Soil Conservation Service, the Hydraulic Laboratory, and the Minnesota Agricultural Experiment Station covering a study of the hydraulics of soil conservation structures. The work was under the immediate direction of Mr. Lewis A. Jones, former Chief of the Division of Drainage and Water Control.

REFERENCES

1. Engineering for Masonry Dams, by William P. Creager, John Wiley and Sons, Inc., New York, 1917, pp. 105-110.
2. Studies of Crests for Overfall Dams, Bureau of Reclamation, U. S. Department of the Interior, Boulder Canyon Project, Part VI—Hydraulic Investigations, 1948.

3. Engineering for Dams, by Julian Hinds, William P. Creager, and Joel D. Justin, John Wiley and Sons, Inc., New York, New York, 1945, p. 362, Table 1.
4. "A Study for the Design of Crests for Overfall Dams," by J. E. Warnock, thesis submitted to the faculty of the Graduate School of the University of Colorado, 1939; laboratory work done by the U. S. Bureau of Reclamation, Denver, Colorado.
5. Handbook of Applied Hydraulics, by Calvin V. Davis, McGraw-Hill Book Company, Inc., 1942, p. 338, Table 1.
6. "On the Form of the Crest Streams," by Ettore Scimemi, L'Energia Elettrica, April, 1930, pp. 293-305.
7. Engineering Hydraulics, by Hunter Rouse, John Wiley and Sons, Inc., New York, New York, 1950, pp. 529-531.
8. Fluid Mechanics for Hydraulic Engineers, by Hunter Rouse, McGraw-Hill Book Company, Inc., 1938.

TABLE I
COMPARISON OF MAPPE EQUATIONS
 $h/H = 0$

Source	C	$\tan \theta$	S/2	T/H
Reference (1), p. 108	0.173	+0.057	-0.3675	0.610
Reference (1), p. 110, Table XVIII	0.190	+0.046	-0.366	0.588
Reference (2), Tables 12 & 18	0.139	+0.085	-0.440	0.538
Reference (3), p. 363	0.153	+0.060	-0.430	--
Reference (5), p. 338	0.024	+0.090	-0.450	0.578
Reference (6), H = 4.4 cm	0.130	+0.050	-0.422	0.593
Reference (6), H = 8.8 cm	0.146	+0.050	-0.414	0.568
Reference (6), H = 13.2 cm	0.146	+0.050	-0.410	0.542
Reference (7), p. 529, Fig. 11	0.198	-0.030	-0.405	0.573
Reference (7), pp. 530-531, Fig. 12	0.190	-0.017	-0.406	0.545
Averages of References (2), (3), (6), (7)	0.157	-0.035	-0.418	0.560
Author	0.150	-0.055	-0.425	0.559

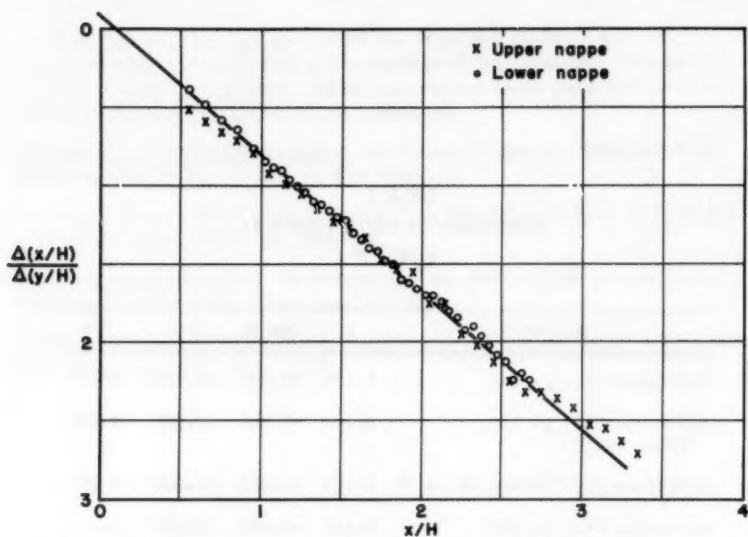
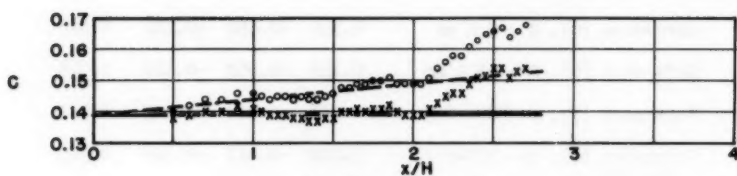
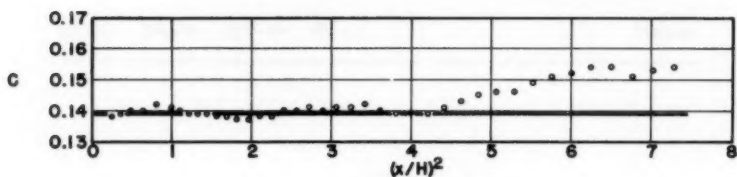


Fig. 1—Typical Plot for the Determination of S and $\tan \theta$



(a) Test of $\tan \theta$

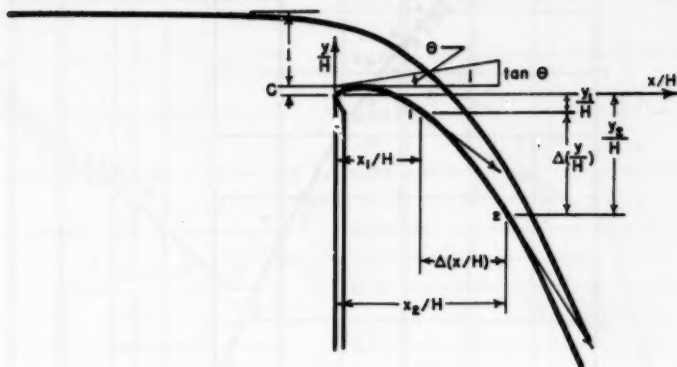
o $\tan \theta = 0.080$ x $\tan \theta = 0.085$



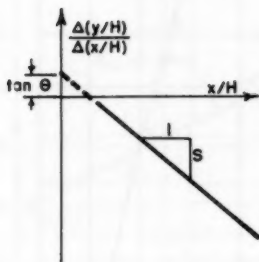
(b) Test of S

$S = 0.88$

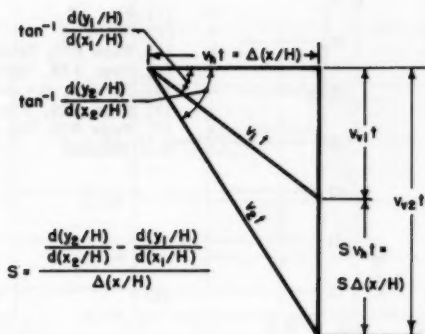
Fig. 2—Tests of S and $\tan \theta$



(a) Section Through Nappe

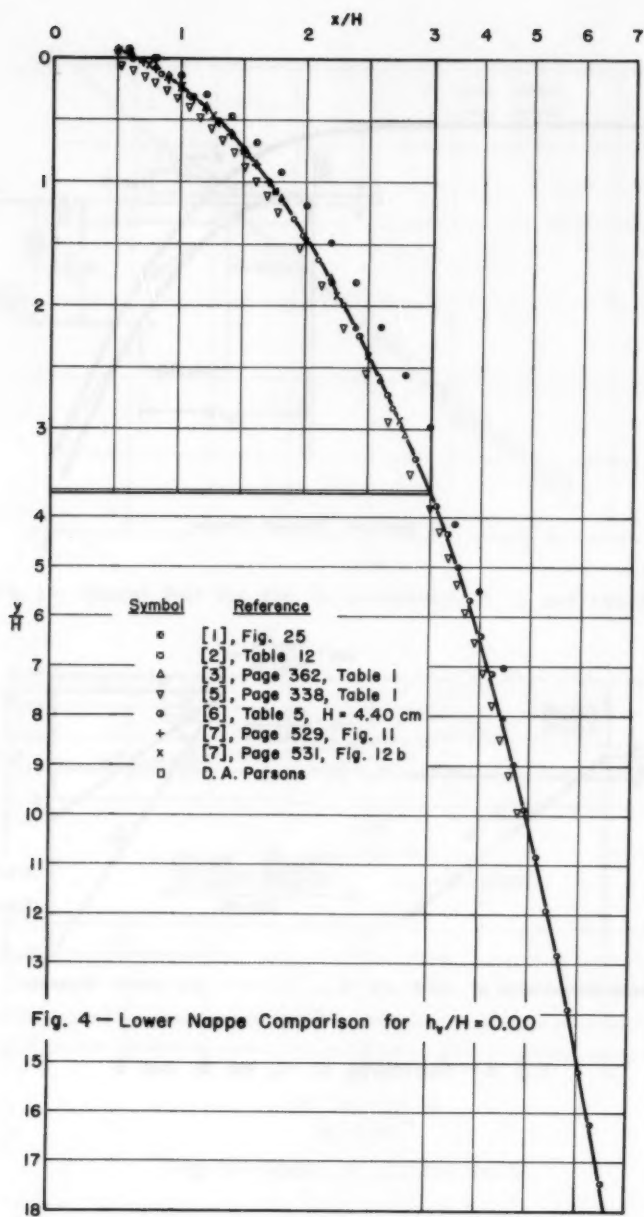


(b) Graphical Determination of $\tan \theta$ and S



(c) Vector Diagram

Fig. 3—Illustration of C , $\tan \theta$, and S



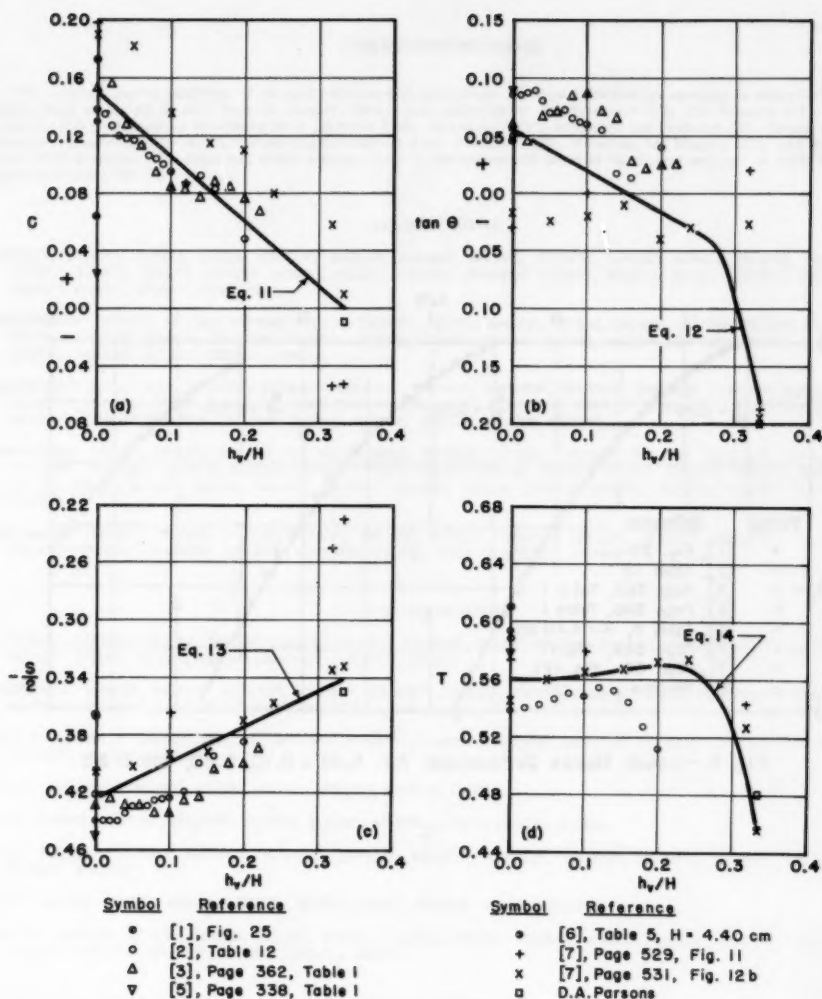


Fig. 5—Effect of Approach Velocity on C , $\tan \theta$, $S/2$, and T

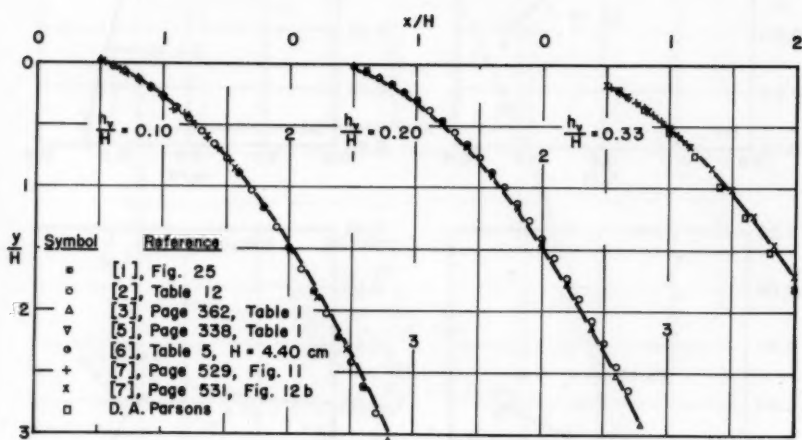


Fig. 6 - Lower Nappe Comparison for $h_v/H = 0.10, 0.20, \text{ and } 0.33$

PROCEEDINGS-SEPARATES

The technical papers published in the past year are presented below. Technical-division sponsorship is indicated by an abbreviation at the end of each Separate Number, the symbols referring to: Air Transport (AT), City Planning (CP), Construction (CO), Engineering Mechanics (EM), Highway (HW), Hydraulics (HY), Irrigation and Drainage (IR), Power (PO), Sanitary Engineering (SA), Soil Mechanics and Foundations (SM), Structural (ST), Surveying and Mapping (SU), and Waterways (WW) divisions. For titles and order coupons, refer to the appropriate issue of "Civil Engineering" or write for a cumulative price list.

VOLUME 79 (1953)

AUGUST: 230(HY), 231(SA), 232(SA), 233(AT), 234(HW), 235(HW), 237(AT), 238(WW), 239(SA), 240(IR), 241(AT), 242(IR), 243(ST), 244(ST), 245(ST), 246(ST), 247(SA), 248(SA), 249(ST), 250(EM)^a, 251(ST), 252(SA), 253(AT), 254(HY), 255(AT), 256(ST), 257(SA), 258(EM), 259(WW).

SEPTEMBER: 260(AT), 261(EM), 262(SM), 263(ST), 264(WW), 265(ST), 266(ST), 267(SA), 268(CO), 269(CO), 270(CO), 271(SU), 272(SA), 273(PO), 274(HY), 275(WW), 276(HW), 277(SU), 278(SU), 279(SA), 280(IR), 281(EM), 282(SU), 283(SA), 284(SU), 285(CP), 286(EM), 287(EM), 288(SA), 289(CO).

OCTOBER:^b 290(all Divs), 291(ST)^a, 292(EM)^a, 293(ST)^a, 294(PO)^a, 295(HY)^a, 296(EM)^a, 297(HY)^a, 298(ST)^a, 299(EM)^a, 300(EM)^a, 301(SA)^a, 302(SA)^a, 303(SA)^a, 304(CO)^a, 305(SU)^a, 306(ST)^a, 307(SA)^a, 308(PO)^a, 309(SA)^a, 310(SA)^a, 311(SM)^a, 312(SA)^a, 313(ST)^a, 314(SA)^a, 315(SM)^a, 316(AT), 317(AT), 318(WW), 319(IR), 320(HW).

NOVEMBER: 321(ST), 322(ST), 323(SM), 324(SM), 325(SM), 326(SM), 327(SM), 328(SM), 329(HW), 330(EM)^a, 331(EM)^a, 332(EM)^a, 333(EM)^a, 334(EM), 335(SA), 336(SA), 337(SA), 338(SA), 339(SA), 340(SA), 341(SA), 342(CO), 343(ST), 344(ST), 345(ST), 346(IR), 347(IR), 348(CO), 349(ST), 350(HW), 351(HW), 352(SA), 353(SU), 354(HY), 355(PO), 356(CO), 357(HW), 358(HY).

DECEMBER: 359(AT), 360(SM), 361(HY), 362(HY), 363(SM), 364(HY), 365(HY), 366(HY), 367(SU)^c, 368(WW)^c, 369(IR), 370(AT)^c, 371(SM)^c, 372(CO)^c, 373(ST)^c, 374(EM)^c, 375(EM), 376(EM), 377(SA)^c, 378(PO)^c.

VOLUME 80 (1954)

JANUARY: 379(SM)^c, 380(HY), 381(HY), 382(HY), 383(HY), 384(HY)^c, 385(SM), 386(SM), 387(EM), 388(SA), 389(SU)^c, 390(HY), 391(IR)^c, 392(SA), 393(SU), 394(AT), 395(SA)^c, 396(EM)^c, 397(ST)^c.

FEBRUARY: 398(IR)^d, 399(SA)^d, 400(CO)^d, 401(SM)^c, 402(AT)^d, 403(AT)^d, 404(IR)^d, 405(PO)^d, 406(AT)^d, 407(SU)^d, 408(SU)^d, 409(WW)^d, 410(AT)^d, 411(SA)^d, 412(PO)^d, 413(HY)^d.

MARCH: 414(WW)^d, 415(SU)^d, 416(SM)^d, 417(SM)^d, 418(AT)^d, 419(SA)^d, 420(SA)^d, 421(AT)^d, 422(SA)^d, 423(CP)^d, 424(AT)^d, 425(SM)^d, 426(IR)^d, 427(WW)^d.

APRIL: 428(HY)^c, 429(EM)^c, 430(ST), 431(HY), 432(HY), 433(HY), 434(ST).

MAY: 435(SM), 436(CP)^c, 437(HY)^c, 438(HY), 439(HY), 440(ST), 441(ST), 442(SA), 443(SA).

JUNE: 444(SM)^e, 445(SM)^e, 446(ST)^e, 447(ST)^e, 448(ST)^e, 449(ST)^e, 450(ST)^e, 451(ST)^e, 452(SA)^e, 453(SA)^e, 454(SA)^e, 455(SA)^e, 456(SM)^e.

JULY: 457(AT), 458(AT), 459(AT)^c, 460(IR), 461(IR), 462(IR), 463(IR)^c, 464(PO), 465(PO)^c.

AUGUST: 466(HY), 467(HY), 468(ST), 469(ST), 470(ST), 471(SA), 472(SA), 473(SA), 474(SA), 475(SM), 476(SM), 477(SM), 478(SM)^c, 479(HY)^c, 480(ST)^c, 481(SA)^c, 482(HY), 483(HY).

a. Presented at the New York (N.Y.) Convention of the Society in October, 1953.

b. Beginning with "Proceedings-Separate No. 290," published in October, 1953, an automatic distribution of papers was inaugurated, as outlined in "Civil Engineering," June, 1953, page 66.

c. Discussion of several papers, grouped by Divisions.

d. Presented at the Atlanta (Ga.) Convention of the Society in February, 1954.

e. Presented at the Atlantic City (N.J.) Convention in June, 1954.

AMERICAN SOCIETY OF CIVIL ENGINEERS

OFFICERS FOR 1954

PRESIDENT

DANIEL VOIERS TERRELL

VICE-PRESIDENTS

Term expires October, 1954:

EDMUND FRIEDMAN
G. BROOKS EARNEST

Term expires October, 1955:

ENOCH R. NEEDLES
MASON G. LOCKWOOD

DIRECTORS

Term expires October, 1954:

WALTER D. BINGER
FRANK A. MARSTON
GEORGE W. McALPIN
JAMES A. HIGGS
I. C. STEELE
WARREN W. PARKS

Term expires October, 1955:

CHARLES B. MOLINEAUX
MERCER J. SHELTON
A. A. K. BOOTH
CARL G. PAULSEN
LLOYD D. KNAPP
GLENN W. HOLCOMB
FRANCIS M. DAWSON

Term expires October, 1956:

WILLIAM S. LaLONDE, JR.
OLIVER W. HARTWELL
THOMAS C. SHEDD
SAMUEL B. MORRIS
ERNEST W. CARLTON
RAYMOND F. DAWSON

PAST-PRESIDENTS

Members of the Board

CARLTON S. PROCTOR

WALTER L. HUBER

EXECUTIVE SECRETARY

WILLIAM N. CAREY

TREASURER

CHARLES E. TROUT

ASSISTANT SECRETARY

E. L. CHANDLER

ASSISTANT TREASURER

GEORGE W. BURPEE

PROCEEDINGS OF THE SOCIETY

HAROLD T. LARSEN

Manager of Technical Publications

DEFOREST A. MATTESON, JR.

Editor of Technical Publications

PAUL A. PARISI

Assoc. Editor of Technical Publications

COMMITTEE ON PUBLICATIONS

FRANK A. MARSTON, *Chairman*

I. C. STEELE

GLENN W. HOLCOMB

ERNEST W. CARLTON

OLIVER W. HARTWELL

SAMUEL B. MORRIS